https://doi.org/10.3311/PPci.23169

Periodica Polytechnica Civil Engineering

Mathematical Modeling of a Corrugated Geogrid and Geocell Reinforced Flexible Pavement Base with Interlayer Shear Performance Analysis

Santosh Kumar[1*], Sanjeev Kumar Suman[1]

[1] Department of Civil Engineering, National Institute of Technology Patna, Ashok Rajpath, Patna, Bihar 800005, India
[*] Corresponding author, e-mail: santoshk.phd18.ce@nitp.ac.in

Received: 09 August 2023, Accepted: 29 December 2023, Published online: 27 March 2024

Abstract

To combat permanent deformation in flexible road pavements and extend lifespan while reducing maintenance costs, an investigated solution "Corrugated Geogrid and Geocell Reinforced Flexible Pavement Base Design" is proposed. It enhances durability by improving inter-layer bonding and increasing the friction coefficient with a Corrugated Imminent Hexagonal Composite Geogrid, boosting pavement bearing capacity. The necessity of this research is the integration of corrugated geogrids and geocells into the design of flexible pavement, in conjunction with a comprehensive evaluation of interlayer shear performance, effectively tackles a range of engineering obstacles and enhances the pavement system's durability, stability, and affordability. Geogrid's corrugated structure resists shoving, offers stabilization, and, combined with Fusion Geoblanket and Perforated Geocell, prevents potholes. Typically, geocellular brace parts are utilized in civil engineering and technical applications, and they are frequently connected to geocellular systems or geocells. These systems are frequently employed in the building of retaining walls, slope protection, erosion control, and soil stabilization. The intended use and product design influence the installation procedures and specific functioning approach. The proposed model prevents permanent pavement failures, ensuring durability, low maintenance, and improved lifespan, assessed through Finite Element Analysis. Thus, the proposed method develops a layout for flexible pavement that's going to prolong its life expectancy and prevent long-term deformation failure.

Keywords

corrugated geogrid, geocell, hexagonal composite geogrid, interlayer shear performance, geocellular brace, finite element analysis, flexible pavement

1 Introduction

Traffic loads are spread across sublayers, and induced loadings are conveyed to the natural subgrade soil via pavement structures. In flexible pavement systems, a base course layer of aggregate materials is frequently deposited on top of naturally occurring subgrade dirt and is followed by a layer of hot mixed asphalt. Pavement engineers have encountered many challenges while planning and constructing flexible pavements on wet natural soils, in high-precipitation areas, and soft soils with insufficient strength. The inability of these natural soils to endure development and transportation pressures is a widespread issue that generates a range of issues [1–3]. Several factors contribute to the deterioration of asphalt pavement, including traffic volume, pavement design, materials, the environment, aging, and so on. Several factors influence the pavement's durability and condition. One of these components that has a considerable impact on pavement performance and makes it difficult to sustain pavement life is traffic loads. While aging and the climate are beyond our control, changing the drainage design is similarly difficult. A present pavement may be protected by taking activities such as managing load constraints, using cautious materials, and using new building methods. The volume of traffic can be controlled to slow pavement degradation. As a result, pavement management must have a better understanding of traffic data and loads [4–6].

The structural characteristics of a pavement (materials and layer thickness, construction quality, maintenance procedures, and subgrade) impact its performance. Flexible pavement bends under traffic pressure, having varying

Cite this article as: Kumar, S., Suman, S. K. "Mathematical Modeling of a Corrugated Geogrid and Geocell Reinforced Flexible Pavement Base with Interlayer Shear Performance Analysis", Periodica Polytechnica Civil Engineering, 2024. https://doi.org/10.3311/PPci.23169

impacts on various strata. Because the strength of each layer changes, the load distribution patterns of flexible pavements differ from one layer to the next. Any weakness in any layer might cause cracking and rutting, eventually leading to the pavement breaking. As a result of climate change, engineering structures must be constructed to meet new load and foundation criteria, as well as statistical river flows. According to recent studies, weather and climate-related risks are the leading causes of civil engineering structural failures and disasters [7, 8]. Without a doubt, the construction sector strongly contributes to human-caused climate change, accounting for around 40% of greenhouse gas emissions, 50% of raw material extraction and consumption, 40% of energy consumption, and 30% of global garbage output. Furthermore, building operations induce eutrophication, acidification, particle formation, ozone depletion, desertification, deforestation, soil erosion, and excessive water resource usage [9, 10].

Civil engineers may significantly minimize the environmental effects of their projects by using innovative materials and technologies, such as minimizing embodied and operational carbon. In addition to garbage from buildings and demolition, waste from other companies can be utilized. Geosynthetics may be employed for the aforementioned purposes in addition to being used in structures that contribute to climate change mitigation. Geosynthetics are often composed of polypropylene (PP), polyethylene terephthalate (PE), and polyethylene (PE), but they can also be composed of natural fibers such as jute, hemp, coir, cotton, sisal, kenaf, wool, straw, and bamboo, as well as biodegradable polymers. They frequently try to improve, change, or retain the properties of the soil with which they interact in civil engineering and building applications. They can be found in the form of fibers, meshes, or laminates, depending on their intended function. Geosynthetics, for example, are used to stabilize slopes, waterproof, separate different types of soil, regulate erosion, and separate waterproofing components. Geosynthetics were also employed to seal the asphalt layer and prevent cracking. Geotextiles, geogrids, and geocomposites are the most often used geosynthetic materials in pavement construction. These materials can be employed in several ways to accomplish one or more specific responsibilities in the context of road construction [11–13].

In comparison to the actual uses of geosynthetic reinforcement, the development of design methodologies and theoretical frameworks for pavement construction has been slow. Researchers often employ many experimental testing approaches to explore various geosynthetics-related characteristics such as embedment location, layer count, layer spacing, shape, and mechanical qualities such as tensile strengths. Damage analysis is performed in line with the maximum surface deflection requirements to calculate the permitted number of load repetitions before pavement failure. A stiffer pavement has less surface deflection and can tolerate more load repetitions before collapsing [14, 15]. Nonetheless, more research on these mathematical models is needed to improve the performance of flexible geosynthetic pavement design, which should eliminate the effects of permanent deformation failure of pavements caused by changing environmental conditions and shifting vehicle loads while also taking inter-layer shear behavior into account.

Major contributions in this study are given as follows:

- To avoid the permanent deformation failure of the flexible pavement and improve its lifetime, a novel Corrugated Imminent Hexagonal Composite Geogrid layer has been proposed which increases the friction coefficient and adds shear resistance to the inter-layer and avoids lateral plastic shear flow thereby mitigating the shoving failure of the pavement.
- To avoid the pothole formation of the top asphalt layer, a Fusion Geoblanket Mounted Perforated Geocellular Brace layer is introduced which provides high crushing strength and avoids fatigue cracking by reducing the distresses to the pavement layers thereby avoiding potholes.
- Furthermore, to analyze the performance of novel pavement design, Finite Element Analysis has been utilized to investigate the interlayer shear performance effect.

These contributions, which were mentioned above, are used to avoid permanent pavement failures such as shoving and potholes and also analyze unique behaviors in the reinforced base layer and interface in the geocell-reinforced flexible pavement. The content of the paper is as follows: Section 2 outlines the literature survey, Section 3 describes the proposed methodology and its working process, and Section 4 provides the proposed model evaluation and performance. Finally, Section 5 brings the paper to the Conclusions.

2 Literature survey

Medjdoub and Abdessemed [16] conducted an experimental investigation involving the application of several geogrid types to asphalt concrete samples. Some specimens were reinforced before loading, while the remainder were

pre-cracked and loaded. They were subjected to static and then cyclic loading. Also considered are the effects of geogrid type, loading type, and frequency. The impacts of cyclic loading and temperature change were investigated by modeling the performance of real pavements in the vast Algerian south, where the thermal gradient can approach 30 °C. Twenty samples were tested to determine their tensile strength, stresses, and strains. A numerical investigation based on the finite element technique was carried out using customized software to match the experimental findings. However, the axial loading effect on the bonding between the geogrid and the pavement layer was not taken into account in the research.

Chua et al. [17] presented ABAQUS finite element methods that were used to assess the bearing capacity of a square footing on an unstabilized and geogrid-stabilized granular layer over clay. The model took into account a range of soil properties and layer thicknesses. The model's two-layered soil structure was built on a strong top granular layer and a weak below clay layer. The finite element analysis parametric findings were used to create design curves with dimensionless parameters in terms of linear gradient and the ratio of the undrained shear strength of clay to the effective vertical stress of the granular layer. The defined design curves were utilized to determine the minimum thickness of the granular layer and are compared to other existing approaches. However, while this study assessed the short-term performance of the geosynthetic-based flexible pavement, the long-term performance must also be assessed for proper analysis.

El-kady et al. [18] analyzed the importance of varied geotextile, geo-foam, and construction and demolition waste combinations for the fortification of soft clay soil. The vertical deformations of railway embankments were calculated using ABAQUS under a moving train load of 125 kN. It also investigated how train speed influenced expected vertical deformation. 3D numerical modeling was performed with varied depths of geo-foam coated with a layer of geotextile on the top surface. FEA was performed using the Modified Cam-Clay model, and the results revealed that reinforcing soft clay with C&D, and geo-foam covered with geotextile decreased the projected vertical deformations. FEA was performed using the Modified Cam-Clay model, and the results revealed that reinforcing soft clay with C&D, and geo-foam covered with geotextile decreased the projected vertical deformations. A field monitoring of a railway segment reinforced with Geo-foam-covered geotextile is still required for a more accurate evaluation of the outcomes.

Zhang et al. [19] investigated the impacts of geocell pocket size, tensile stiffness, and peak internal frictional angle on the stress-strain responses of geocell-reinforced surface-base milling mixes. Stability analysis was done on the geocell-reinforced retaining wall with surface-base milling mixes using the finite element strength reduction technique to examine the factor of safety and the failure cause of the structure. Surface milling materials demonstrated strain hardening, whereas gravel and surface-base milling combinations indicated strain softening. However, the qualities of the filler material in the geocell must be researched further for optimum resource usage.

Ruiz et al. [20] offered a mathematical technique for the fatigue study of flexible pavements that considered the effects of dynamic axle loads. The IRI (International Roughness Index) increases with time in a pavement degradation model. Time is broken down into separate time increments. A function in a road surface generation model generates the proper IRI value for each time step. A QHV (Quarter Heavy Vehicle) model supplied the dynamic amplification function for the stresses imposed on the road surface during a simulated ride. This function could be easily averaged, providing the effective dynamic load amplification factor (DLA), which was the ratio of effective dynamic loading to static loading at each time step. However, to increase the trustworthiness of the data acquired, standardized testing techniques must be developed.

Yin et al. [21] conducted a computational analysis of low-volume flexible pavement reinforced with geotextile material under static stress was carried out to assess the improvement due to reinforcement based on three criteria: rutting performance, geosynthetic installation location, and base course thickness reduction. The Finite Element Method (FEM) was used to model three-dimensionally in Abaqus/CAE software. Geotextile reinforcement at the base-subgrade and AC-base interfaces decreased rutting by up to 25.2% for the unreinforced pavement system, according to the research. The elastic modulus of the geosynthetic material, installation location, and several reinforcing layers all have an impact on the pavement system's deflection response behavior. However, the load transfer mechanisms between the geosynthetic and pavement layers must also be investigated to have a better knowledge of the pavement's overall performance.

Wang et al. [22] conducted a preliminary research study that evaluated the reinforcing efficiency of asphalt pavement reinforced with geocell. The longitudinal strain peak value of the pavement structure reinforced with Polypropylene geocell was much lower in comparison

to the pavement response without geocell, according to field experiment findings. The reinforcing system inhibited creep strain, and the improvement factor increased with increasing axle load and decreased with increasing speed. Polypropylene has superior temperature tolerance than Polyethylene and Polyethylene Terephthalate and is ideal as a geocell material in asphalt pavement structures. The PP geocell is determined to be successful in limiting the peak of longitudinal strain at the bottom of the asphalt layer reinforced by geocell based on the dynamic test results of the testing pavement construction. However, the vehicle speed increases and the reinforcing effect reduces.

Liu et al. [23] investigate a method of structural parameter correction in semi-rigid base asphalt pavement combining numerical simulations, laboratory tests, and accelerated pavement testing (APT) was proposed to address the issue that material parameters measured under specific laboratory conditions are extremely different from the actual pavement. Temperature, size, and fatigue were investigated using dynamic modulus and uniaxial static compression creep experiments. The inversion results of pavement structural parameters based on three-dimensional FE simulation show that there were noticeable differences between the material parameters in laboratory testing and the actual pavement, and the differences varied with temperature, size, and frequency in various forms.

Beyene [24] This study attempts to create such a concept. The influence of material property and pavement layer thickness on the response of a flexible pavement construction is investigated using a finite-element approach and the ABAQUS software package. The asphalt, base course, subbase, and subgrade layers of flexible pavement were subjected to stress-strain and deflection evaluations. The finite-element calculations revealed that rutting deformation is caused by vertical compressive stress at the subgrade layer, while fatigue cracking is caused by horizontal tensile strain at the base course and subbase layer. The reasons that induced discomfort are repeated loading, the strength and quality of the base course, subbase, and subgrade layer materials. However, Instability in any of the layers will cause the paving system to fail and each layer must be carefully and precisely constructed.

Menon et al. [25] investigate the scaled model experiments employing the unit cell concept carried out in a soft clayey subgrade to investigate the effect of conventional and enclosed stone columns on subgrade behavior. Furthermore, the additional enhancement of strengthening the granular basis with geocell was studied utilizing four different materials, including waste rubber tire crumbs. The frictional properties of the infill material influence the behavior of geocell-reinforced ground to a small amount, with the effect being more obvious at higher stress levels. Partially replacing conventional granular materials like sand/fine aggregate with the optimal amount of rubber tire crumbs of equivalent gradation improves system performance at higher stress levels. However, the effect of encasement is directly affected by the stiffness of the fabric.

Matveev et al. [26] The design model of a reinforced crushed stone layer calculated as a multilayer plate on an elastic base using the technical theory of bending and the Bubnov-Galerkin method is proposed, allowing the effectiveness of using various types of geosynthetic materials for reinforcing granular pavement bases to be theoretically calculated and justified. The model is based on the concept that the mechanical connection with the geogrid causes the reinforced granular layer to flex like a plate on an elastic foundation. The pavement structure's reinforced granular basis was designed as an equivalent in stiffness two-layer bending plate on an elastic base. The cylindrical stiffness formulae for a two-layer plate are obtained. They define the stiffness properties of each layer as well as the entire bundle of layers. However, it is not possible to use it in actual calculations of the bases of granular materials reinforced with geogrid.

Mahgoub and El Naggar [27] proposed a coupled TDA–geocell stress-bridging system to build using a thorough three-dimensional (3D) finite-element modeling component and six full-scale tests. However, lightweight compressible materials could cause unfavorable surface settling, which could impair the functionality of the pipe. The devised solution reduces the applied loads on the pipe below and controls surface settling by inducing a stress-arching mechanism over the TDA layer with a top granular backfill layer reinforced with geocells. Innovative systems may not perform well in the long run, especially if they lack a proven track record. Therefore, it is crucial to consider the system's longevity and dependability.

Saride et al. [28], used monotonic loading tests to determine the installation depth of geogrid- and geocell-reinforced base courses for flexible pavements. The Modulus Improvement Factor (MIF), which ranges for both geogrid and geocell-reinforced bases, was used in this research to quantify structural support. Base-layer coefficients were obtained for these reinforcements following a methodical investigation. Verification using an as-built pavement from Montana and current methods revealed that

layers reinforced with geogrid and geocells were thinner. However, there's a chance that the results of the research apply very far, therefore more testing in various scenarios was likely needed.

Khorsandiardebili and Ghazavi [29], used the Limit Equilibrium Method and the Horizontal Slice Method to research the stability of slopes reinforced with geocells. They developed a formula for geocell-reinforced slope analysis based on pertinent equilibrium equations, introducing a specific analytical framework. Research using parametric analysis assessed the effects of changing the height of the geocell and replacing geogrids with geocells on slopes with different properties. The results indicated possible reductions in the length of the reinforcement layer and the amount of tension needed, improving stability conditions. However, the research's sensitivity to certain circumstances was noted, as the requirement for additional validation before it became used more widely.

Sitharam and Gupta [30] investigated the behavior of soil with and without geocell confinement in model test tests on clay beds reinforced with geocells. Utilizing FLAC 3D, three-dimensional numerical simulations were run and verified against experimental findings. The Mohr – Coulomb model represented the infill material (coarse sand), while the Modified Cam Clay model approximated the behavior of the clay bed. The goal of the research was to comprehend interference effects and establish the ideal footing spacing for clay beds that were neither geocell-reinforced nor unreinforced. However, the interference effect was more noticeable in geocell-reinforced clay than in geogrid-reinforced clay, indicating possible difficulties or restrictions in specific situations that call for more research and thought.

Ari and Misir [31] investigated to determine how well geocell reinforcement works to lessen settlement and increase the bearing capacity of conical and pyramidal shell foundations. As shell foundations, conical and pyramidal geometries were employed, and PLAXIS 3D was used to replicate their actual honeycomb structures. Data from several laboratory investigations published in the literature were used to independently validate numerical models for shell foundations and geocell-reinforced foundations. The behavior of shell foundations lying on sandy soils reinforced with geocell was subsequently examined using the expanded, verified models. It's important to remember that this research's application is restricted to particular circumstances, and additional testing in a variety of settings is necessary to validate geocell reinforcement's wider efficacy.

Overall from this literature study, it is understood that [16] did not consider the axial loading effect on the bonding between the geogrid and pavement layer, [17] the long-term performance also needs to be evaluated for the proper analysis, [18] a field monitoring of a railway section reinforced with geosynthetics is needed, [19] the properties of the filling material in the geocell need to be further studied, [20] the development of standardized testing methods is necessary, [21] the load transfer mechanisms between the geosynthetic and pavement layers also need to be studied, [22] the vehicle speed increases and the reinforcing effect reduces in asphalt layer, [23] instability in any of the layers will cause the paving system to fail, and in [25] the effect of encasement is directly affected by the stiffness of the fabric and in [26] it is not possible to use it in actual calculations. In [27] the need to improve the system's longevity and dependability, [28] more testing in various scenarios was likely needed, [29] requirement for additional validation used more widely, [30] interference effect causes potential challenges in specific situations, requiring further research, [31] necessary to validate geocell reinforcement's wider efficacy. Therefore, there is a need for a novel flexible pavement design using geosynthetic material with proper mathematical analysis to eliminate these limitations.

3 Mathematical modeling of a corrugated geogrid and geocell reinforced flexible pavement design

A highway pavement is a structure made up of stacked layers of processed materials that are placed on top of a natural soil subgrade, with the primary function of distributing applied vehicle loads to the subgrade. Geosynthetics are increasingly used to extend the life and performance of pavements. Permanent deformation is a major cause of concern for flexible road pavements, and it must be minimized to extend their life and save money on maintenance. The existing flexible pavement design approaches still cannot eliminate the major permanent deformation failures such as shoving and pothole formation and thus have a limited life span. Hence a novel Corrugated Geogrid and Geocell Reinforced Flexible Pavement Base with Interlayer Shear Performance Analysis is proposed, to avoid the permanent deformation failure of the flexible pavement and improve its lifetime. Shoving is a type of permanent deformation in which bulges and ripples are formed across the pavement by the lateral plastic shear flow of the pavement surface. The existing studies did not consider the relative displacement of the binder course and

the base layer due to a lack of bonding and the inter-layer horizontal shear stress which is also an important factor that causes shoving. Hence a novel Corrugated Imminent Hexagonal Composite Geogrid is introduced in between the binder course and the base layer. This hexagonal composite geogrid is made of high-strength steel coated with polypropylene, which increases the friction coefficient between the layer material while also improving inter-layer bonding and therefore increasing the bearing capacity of the layer. The corrugated structure of this proposed geogrid provides additional shear resistance to the inter-layer and avoids lateral plastic shear flow thereby mitigating the shoving failure of the pavement.

Some of the existing studies use air-entrained asphalt mixes to mitigate the effects of freeze-thaw cycles on pavement performance but, air voids naturally form in the asphalt mixture during production and placement which makes it unnecessary to provide air entrainment in this asphalt layer. Additionally, the use of air-entraining agents increases the porosity of the asphalt layer thereby reducing the strength-to-weight ratio (*S*/*W* ratio) and increasing the surface wear of the layer material. Also, the existing studies did not consider a base layer design without air entrainment to avoid the pothole formation of the top asphalt layer To address this issue, a novel Fusion Geoblanket Mounted Perforated Geocellular Brace is introduced in the base layer of the pavement. The Fusion Geoblanket Composite Mat is a geotextile comprised of warp-knitted thermally treated Aramid Fibres and Polyester that is introduced between the base layer and the subgrade. Because of the presence of Aramid fibers, this geoblanket has a high crushing strength and a strong resistance to stretching and shrinking. On top of this geoblanket is a Perforated Geocell made of high-density polyethylene (HDPE), the cells are filled with fine gravel pebbles (size equal to or less than 5 mm), naturally forming air gaps without the need for any air entrainment agents. These natural air gaps, in conjunction with the perforations on the geocell, give free space for the freeze-thaw cycle and prevent fatigue cracking by lowering distresses to the pavement layers, hence eliminating potholes. Furthermore, because these Geocells disperse the pressure over a broader area, they can withstand static and dynamic loads on even the weakest subgrade soils. Finally, using Finite Element Analysis, a mathematical model of the proposed pavement design is built and examined in the ABAQUS application, and the following analysis is performed:

1. The suggested flexible pavement's mid-plane is subjected to a high axial load, and the stress distribution is studied with and without the Fusion Geoblanket Mounted Perforated Geocellular Brace.
2. The surface course is subjected to horizontal and inclined stresses, and shear stress fluctuation at the interface of the binder course and base layer is examined with and without the corrugated composite geogrid.

Fig. 1 shows the layers of Corrugated Geogrid and Geocell Reinforced Flexible Pavement Design. The above pavement design contains an asphalt layer, base layer, perforated HDPE geocell and corrugated imminent hexagonal composite geogrid. The structure of flexible pavement is typically made up of the following layers such as the surface course (layer), which is the top layer of flexible

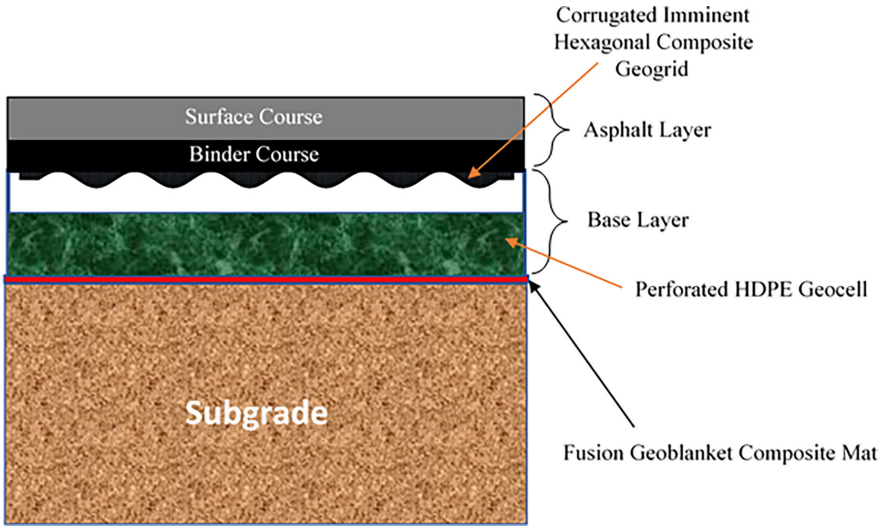

Fig. 1 Corrugated geogrid and geocell reinforced flexible pavement design

pavement, offers the smooth, resilient, and abrasion-resistant qualities of a good roadway while maintaining enough friction for safe driving. Usually, asphalt concrete, which is aggregate bound in bitumen, is used to make it. The binder course is an intermediate, bitumen-bound aggregate layer placed between the base layer and the surfacing of asphalt pavement. The base layer consists of cement-bound aggregate. Polypropylene is frequently used in the production of hexagonal composite geogrids. They are created by heat-welding strips of material, weaving or knitting yarns, or punching holes in sheets of material that are subsequently stretched into a grid. Hexagonal shape describes it. Fusion Geoblanket Composite Mat is produced from two or more constituent materials. Perforated HDPE Geocells improve soil stabilization, load transfer, and erosion control to lower the risk of structural failures. Geocells increase the slopes' resistance to erosive forces and prevent platform settling and deformation. So, these layers were included in the novel flexible pavement design to improve its performance.

3.1 Corrugated imminent hexagonal composite geogrid

Corrugated Imminent Hexagonal Composite Geogrid is introduced in between the binder course and the base layer to avoid permanent deformation failure such as shoving and potholes formation of the flexible pavement and to increase its lifespan. Geosynthetics used for ground reinforcement, such as geogrids, geotextiles, and geocomposites, reduce the thickness of the bearing layer, reduce the use of traditional materials, lower construction costs, and increase the reliability, durability, and performance of earthen structures. The Hexagonal Composite Geogrid layer used in the proposed flexible pavement design is shown in Fig. 2.

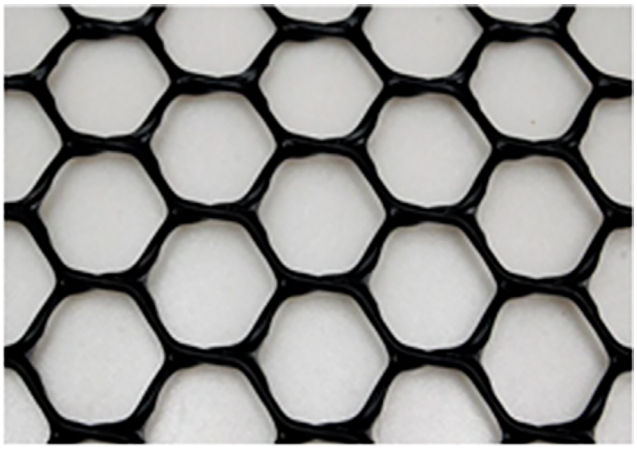

Fig. 2 Hexagonal composite geogrid

Fig. 2 shows the Hexagonal Composite Geogrid layer of the flexible pavement design. It is made from an extruded homo- or copolymer polypropylene sheet that is punched and orientated in three equilateral orientations, resulting in ribs with a high degree of molecular orientation that extends through the bulk of the integral node. This hexagonal composite geogrid is comprised of polypropylene-coated high-strength steel which increases the friction coefficient between the geogrid and layer material. The friction coefficient is given in Eq. (1)

$$f^* = \frac{P_R}{2L\sigma_V'}, \tag{1}$$

where f^* is friction coefficient, P_R is the pull-out force per unit width, L is the length of the reinforcement's binding area and σ_V' effective normal stress.

Geotextile materials' primary function is to aid in the reduction of stresses and deformations. Geogrids placed between the subsoil and base course raise the bearing limit. The interaction of the distributed soil with the geogrid causes healthier inter-layer bonding, which serves to boost bearing capacity and, for the most part, accounts for a reduction in base course thickness. The increased bearing capacity is expressed in Eq. (2)

$$\Delta q_T = \sum_{i=1}^{N} \frac{4T_i\left[u+(i-1)h\right]}{B^2}, \tag{2}$$

where the basic parameters of Eq. (2) include the tensile strength T_i, the width of the base layer is denoted by B, the geogrid layer number is denoted by N, and the vertical spacing between geogrid layers is denoted by h. The ultimate bearing capacity of the strip base on geogrid-reinforced material is given in Eq. (3),

$$q_{ur} = cN_c + qN_q + 0.5\gamma SN_\gamma + \sum_{i=1}^{N} \frac{4T_i\left[u+(i-1)h\right]}{B^2} \tag{3}$$

where q_{ur} denotes the ultimate bearing capacity of the strip based on geogrid-reinforced material, N_c, N_q, and N_γ indicate the bearing capacity factors, ∅ is the internal friction angle, c is the cohesive shear strength, B is the width of the base layer, and q denotes the surcharge loading. One of the key reinforcing processes connected with flexible pavements is ‚increased bearing capacity'. The enhanced bearing capacity mechanism in the presence of geosynthetics leads to soil reinforcement, which finally forces the creation of an alternate failure surface. This new alternate plane is responsible for the increased bearing capacity.

The shear strain delivered to the subgrade is reduced by the reinforcement supplied by geosynthetics. Hence, the corrugated structure of this proposed geogrid provides additional shear resistance to the inter-layer. Shear stress occurs when the weight on the pavement exceeds the pavement's capacity. The movement in the base layer causes shear stress on the top pavement layers. This occurs as the load nears the critical threshold. To improve the shear strength of asphalt mixes, efforts should be made to increase asphalt binder cohesion and aggregate internal friction angle. Because the aggregates' cohesiveness is so poor, shear strength is heavily dependent on inner particle friction and movement resistance. In general, asphalt mixes with better aggregate-binder adhesion create greater rutting resistance. The corrugated structure of this suggested geogrid adds shear resistance to the inter-layer and prevents lateral plastic shear flow, reducing pavement shoving failure. However, permanent deformation failure has to consider potholes which are bowl-shaped deformations formed on the surface of the pavement caused by the distressed fatigue cracks due to water infiltration and the freeze-thaw cycle which are reduced using Fusion Geoblanket Mounted Perforated Geocellular Brace that is explained in next subsection.

3.2 Fusion geoblanket mounted perforated geocellular brace

Fusion Geoblanket Mounted Perforated Geocellular Brace is configured in the pavement's base layer. The Fusion Geoblanket Composite Mat is a geotextile made of thermally treated Aramid Fibres and Polyester in a warp-knitted manner and is provided in between the base layer and the subgrade.

Fig. 3 shows the Wrap Knitted Fusion Geoblanket Composite Mat layer of the flexible pavement design. Fusion Geoblanket Composite Mat is produced from two or more constituent materials. In this materials such as aramid fiber and polyester have notably dissimilar chemical or physical properties and are merged to create a material with properties unlike the individual elements. The application of air-entraining chemicals increases the porosity of the asphalt layer, lowering the strength-to-weight ratio (*S*/*W* ratio). Aramid fiber was the first organic fiber with a high enough tensile modulus and strength to be used as a support material in composite materials. Aramid fibers are designed to be heat and flame-resistant, and they keep these properties even at high temperatures. The term "aramid" refers to aromatic polyamide fibers in which at least 85%

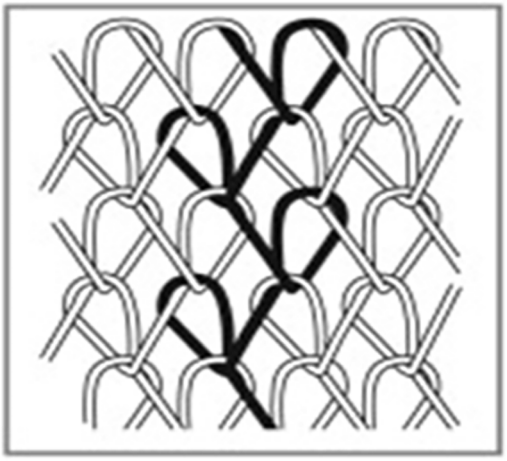

Fig. 3 Wrap knitted fusion geoblanket composite mat

of the amide bonds (—CO—NH—) are directly bonded to two aromatic rings. The polymer is classified based on the para/meta orientation of these bonds. Because of the inclusion of Aramid fibers, this blanket offers a great *S*/*W* ratio. The presence of polyester in the interface shear resistance of fiber/soil is principally determined by the soil particle rearrangement resistance, effective interface contact area, fiber surface roughness, and soil composition. When dirt is reinforced with polypropylene, the unconfined crushing strength is improved, and the shrinkage and swelling properties of clay are decreased. The resistance to shrinkage and conductivity of soil increase as the fiber concentration increases. Shrinkage is expressed in Eq. (4),

$$\alpha_d = \frac{\varepsilon}{\omega} = \frac{\left(\sum_{j=1}^{4} X_{i,j} - \sum_{j=1}^{4} X_{i+1,j}\right) \Big/ 2l}{\left(m_i - m_{i+1}\right) \Big/ m_p} \tag{4}$$

where α_d is the shrinkage coefficient; ε is the shrinkage strain, ω is the water loss rate; m_i and $m_i + 1$ are the weighting mass of the sample in the i^{th} and $(i + 1)^{\text{th}}$ testing respectively; $X_{i,j}$ and $X_{i+1,j}$ is the reading of the j^{th} dial gauge in the i^{th} and $(i + 1)^{\text{th}}$ test respectively; l is the length; m_p is the mass of the sample after drying. Shrinkage causes a garment to be too tight, too loose, too short, or too long, compromising its comfort and functionality. Shrinkage also changes a garment's curve or profile, making it more or less flattering. Furthermore, shrinkage alters a fabric's elasticity or rebound, making it more or less robust or flexible. Air-entrained asphalt mixes mitigate the effects of freeze-thaw cycles on pavement performance but, air voids naturally form in the asphalt mixture during production and placement which makes it unnecessary to provide air entrainment in this asphalt layer. Hence Perforated HDPE Geocell is used which is shown in Fig. 4.

Fig. 4 Perforated HDPE geocell

Fig. 4 shows the Perforated HDPE Geocell layer of the flexible pavement design. Geocells are three-dimensional, expandable panels made of high-density polyethylene, polyester, or other polymeric materials. Perforated geocells have uniform holes in the cell walls that improve stress distribution and reduce deformation. This is done through a large number of edges that turn into cells. The integrity of the geocell depends on the strength of the perforated strip and weld. On top of this geoblanket is a Perforated Geocell constructed of high-density polyethylene, with the cells filled with fine gravel pebbles (size equal to or less than 5 mm), naturally producing air gaps without the need for any air entrainment agents. These natural air spaces, together with the geocell's perforations, give open room for the freeze-thaw cycle. It is often assumed that heavy vehicles are the primary cause of fatigue damage on flexible pavements. The fatigue damage equation is used to predict the fatigue cracking life of flexible pavements is described in Eq. (5),

$$Y = k_1 \left(\frac{1}{\varepsilon_t}\right)^{k_2} \left(\frac{1}{E}\right)^{k_3} \tag{5}$$

where Y represents the load repetitions to cause failure, ε_t is the maximum tensile strain at the bottom of the asphalt layer, E stands for the stiffness modulus of the asphalt layer and k_1, k_2 and k_3 represent the material coefficient.

Fatigue is seen as a damage accumulation process in which the material property deteriorates continually when loads are applied. The damage index, according to Palmgren-Miner's hypothesis, is stated in Eq. (6):

$$D = \frac{X}{Y}, \tag{6}$$

where D is the damage index. Y is the the load repetitions to cause failure and X represents the equivalent number of actual traffic load repetitions applied over the design period of the road section. Considering compound traffic growth. The damage index D is considered as the ratio of two random variables X and Y whose joint probability function is defined in Eq. (7)

$$f_{X,Y} = P\left(X = x, Y = y\right), \tag{7}$$

where $x > 0$, $y > 0$ and $f_{X,Y}(x,y)$ represents the probability that events X and Y are at the same time.

According to Miner's law, fatigue cracking takes place when damage D reaches or exceeds unity. In other words, fatigue cracking takes place as the probability of damage index becomes greater than one. The expression shown in Eqs. (8) and (9)

$$\mathrm{FC} = P\left(D > 1\right) = 1 - P\left(P \le 1\right) \tag{8}$$

$$\mathrm{FC} = \int_1^{\infty} f_D\left(d\right)\mathrm{d}d = 1 - \mathrm{CDF}\left(D \le 1\right), \tag{9}$$

where FC represents fatigue cracking. Also, natural air voids along with the perforations avoid fatigue cracking by reducing the distress to the pavement layers thereby avoiding. The roughness of the road causes extra weight on each wheel. The distribution has a mean value, $\bar{F}$, which is commonly believed to represent the static load and σ standard deviation. The dynamic load coefficient (DLC) is a dimensionless quantity that may be calculated by dividing the standard deviation by the mean static load. This connection is represented mathematically in Eq. (10):

$$\mathrm{DLC} = \frac{\sigma}{\bar{F}}. \tag{10}$$

The DLC concept determines the probability size of the dynamic axle load for a given vehicle speed and road roughness. In theory, a truck traveling on smooth pavement should have a DLC around zero. If N measurements of tire forces, f_k, are available, σ is derived from Eq. (10) and σ^2 is expressed in Eq. (11)

$$\sigma^2 = \frac{1}{N}\sum_{k=1}^{N} f_k^2 \,. \tag{11}$$

The dynamic impact factor, DI, which can be multiplied by the static load to determine the dynamic load due to vehicle-pavement interaction, is estimated from is given in Eq. (12)

$$\mathrm{DI} = 1 + Z_r \times \mathrm{DLC}\,, \tag{12}$$

where Z_r is reliability index considered. It was discovered that when vehicle speed rises, the dynamic impact increases

dramatically. Furthermore, the suspension damping coefficient had a substantial influence on the DI, especially as speed increased. Additionally, these Geocells distribute the load over a larger area and thus are also used to support static and dynamic loads on even weak subgrade soils.

A mathematical model of this proposed pavement design is created and analyzed using the Finite Element Analysis in the ABAQUS tool. A 3D finite-element model was created using the ABAQUS finite-element software program to study the influence of geosynthetic reinforcement in the base course layer on the structural response of a flexible pavement system. The pavement structure's reaction was investigated by placing a geocell reinforcement layer at the bottom of the base course layer. The ABAQUS contact interaction feature was used to model the geosynthetic-soil interface. The ABAQUS contact interaction feature models the interaction of two deformable bodies or a deformable body and a stiff body in two and three dimensions using the constraint technique. The ABAQUS program uses finite element analysis to create and analyze a mathematical model of the proposed pavement design, and the following analysis is carried out:

1. The proposed flexible pavement's mid-plane is subjected to a significant axial load, and the stress distribution is assessed both with and without the Fusion Geoblanket Mounted Perforated Geocellular Brace.
2. Shear stress variation at the interface of the binder course and base layer is examined with and without the corrugated composite geogrid. Horizontal and inclined forces are applied to the surface course.

Overall a novel flexible pavement design base with an efficient mathematical modeling approach has been proposed and designed using a finite element model (FEM) using the ABAQUS tool, the permanent failure of pavements such as shoving and potholes are avoided and this design enables the pavement for heavy traffic with minimized maintenance and an improved lifetime and its performance is analyzed using the mathematical model.

4 Result and discussion

This section provides an experimental setup, the Stimulated output of the proposed model, the performance of the proposed system, and a comparison of the proposed model with existing techniques.

4.1 Experimental setup

Platform: ABAQUS
OS: Windows 10 (64-bit)
Processor: Intel i5
RAM: 8 GB RAM

4.2 Simulation of the proposed system

This section interprets and analyses an effective mathematical modeling strategy that uses ABAQUS' finite element model (FEM).

Fig. 5 depicts the simulated view of the Hexagonal Composite Geogrid layer in the pavement design with measurements. This hexagonal composite geogrid is comprised of high-strength steel that has been coated with polypropylene to enhance the friction coefficient between

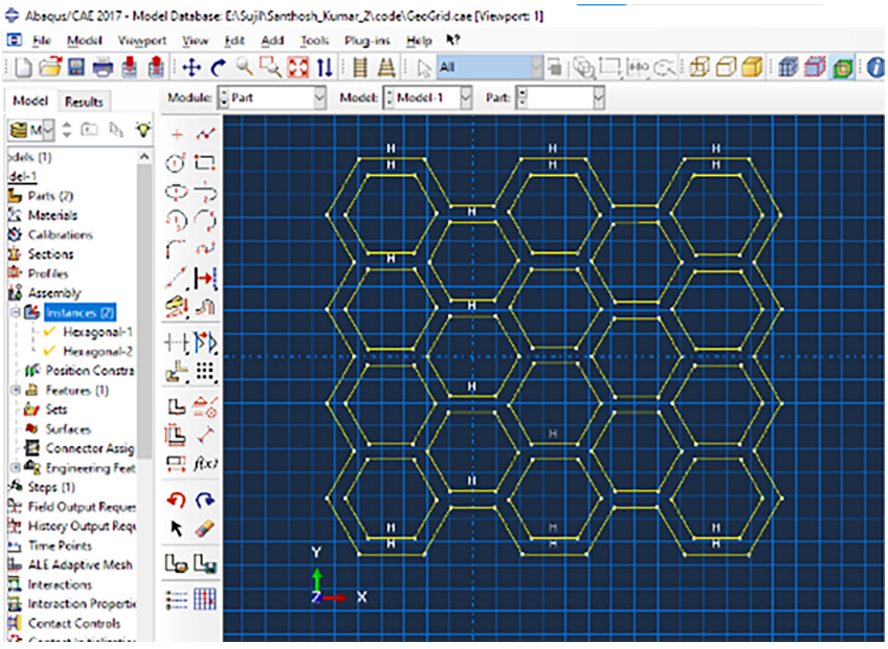

Fig. 5 Simulated view of hexagonal composite geogrid layer

the geogrid and the material of the layer and to promote healthy inter-layer bonding, which boosts the layer's bearing capacity.

The Fig. 6 shows the simulated view of the perforated HDPE Geocell layer of the flexible pavement design. High-density polyethylene (HDPE) perforated geocell is used, and the cells are filled with fine gravel aggregates to naturally create air gaps without the need for air entrainment agents.

The Fig. 7 shows the simulated view of the Wrap-knitted fusion Geoblanket Composite Mat layer of flexible pavement design. The Fusion Geoblanket Composite Mat is a geotextile that is used between the base layer and the subgrade. It is constructed of thermally treated polyester and aramid fibers using a warp-knitted construction. Due to the combination of Aramid fibers and Polyester, this geoblanket has a high crushing strength and a strong resistance to stretching and shrinking.

Fig. 8 illustrates the simulated view of a novel flexible pavement design. The ABAQUS tool's dynamic cyclic loading mode, where the load archives +2.025e -01 mises. The deformation scale factor is +6.405e+02. Fig. 8 also depicts the movement of tires on pavement surfaces.

4.3 Performances metrics of the proposed system

The Performance metrics of the proposed Mathematical model of a Corrugated Geogrid and Geocell Reinforced Flexible Pavement Base with Interlayer Shear Performance Analysis and the achieved outcome were explained in detail in this section.

The Fig. 9 shows the performance of fatigue damage. When load increases fatigue damage also increases. Potholes are bowl-shaped deformations developed on the pavement's surface as a result of disturbed fatigue cracks brought on by water infiltration and the freeze-thaw cycle, which are lessened by the application of Fusion Geoblanket Mounted Perforated Geocellular Brace. By minimizing the distresses to the pavement layers, natural air spaces, and perforations together prevent fatigue cracking. The minimum fatigue damage of 0.32 is attained when the load is 200 Pa. The maximum fatigue damage of 0.45 when the load value is 1000 Pa.

The Fig. 10 shows the performance of deformation. When the load increases deformation also increases for flexible road pavements, permanent deformation is a serious source of worry. The main goal of geotextile materials is to lessen stresses and deformations. Uniform perforations in the cell walls of perforated geocells increase load distribution and lessen distortion. The minimum deformation of 44.5 N when the load is 200 Pa. The maximum fatigue damage of 56 N when the load value is 1000 Pa.

The Fig. 11 shows the performance of shear stress. When load increases shear-stress also increases. When the weight on the pavement is greater than what the pavement can support, shear stress results. The upper pavement

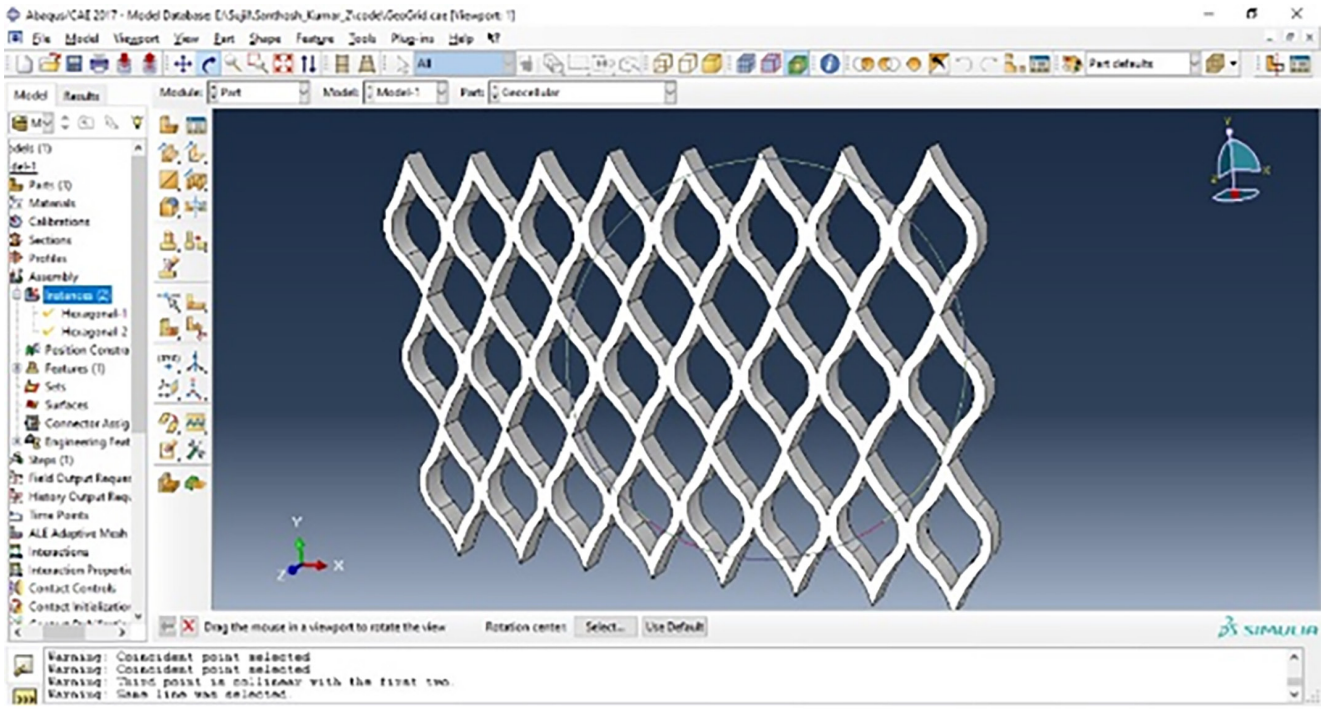

Fig. 6 Simulated view of perforated HDPE geocell layer

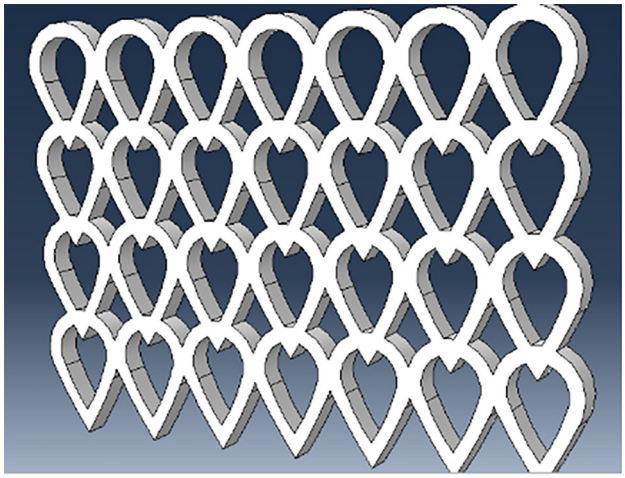

Fig. 7 Simulated view of wrap-knitted fusion geoblanket composite mat layer of pavement design

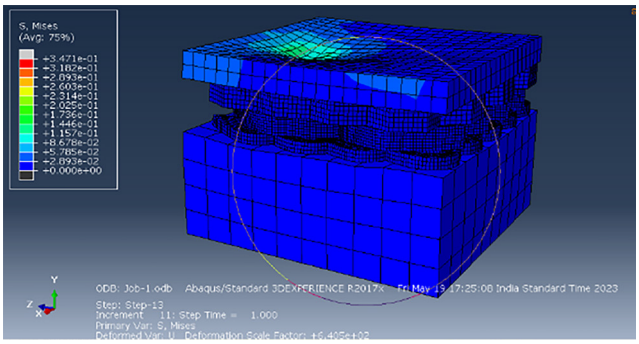

Fig. 8 Simulated view of novel flexible pavement design

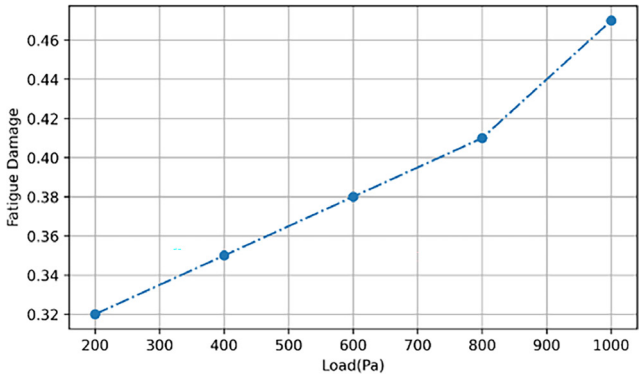

Fig. 9 Performance of fatigue damage

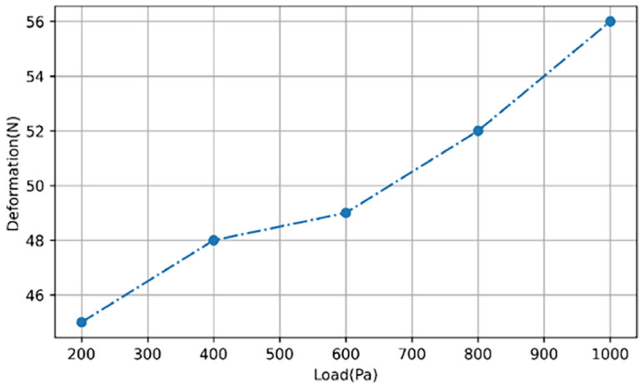

Fig. 10 Performance of deformation

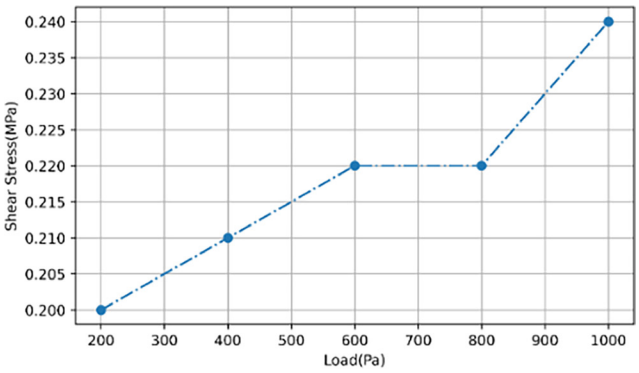

Fig. 11 Performance of shear-stress

layers experience shear stress as a result of the movement of the base layer. The minimum shear-stress of 0.23 MPa when the load is 200 Pa. The maximum shear-stress of 0.24 MPa when the load value is 1000 Pa.

The Fig. 12 shows the performance of rutting in pavement design. When load increases rutting also increases. An increase in aggregate internal friction angle and asphalt binder cohesion has been achieved in the proposed design to boost the shear strength of asphalt mixtures. Shear strength significantly depends on inner particle friction and movement resistance due to the aggregates' low cohesion. Hence, rutting resistance is higher in the proposed design due to the presence of the Fusion Geoblanket Composite Mat. The minimum rutting of 8 mm when the load is 200 Pa. The maximum rutting of 15 mm when the load value is 1000 Pa.

The Fig. 13 shows the performance of wheel load in pavement design. When deflection increases the wheel load also increases. The amount of wheel traffic on the pavement is a crucial consideration when choosing the pavement thickness. This proposed design demonstrates how the distribution of loads may impact deflection and carrying capacity as a whole using Finite element analysis. The minimum wheel load of 1000 Ibf when the deflection is 2 in. The maximum wheel load of 1800 Ibf when the deflection is 10 in.

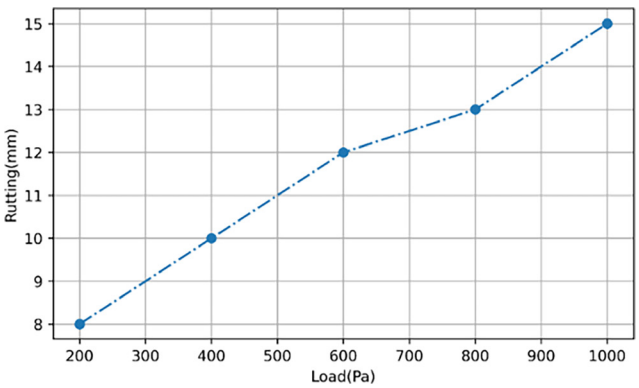

Fig. 12 Performance of rutting

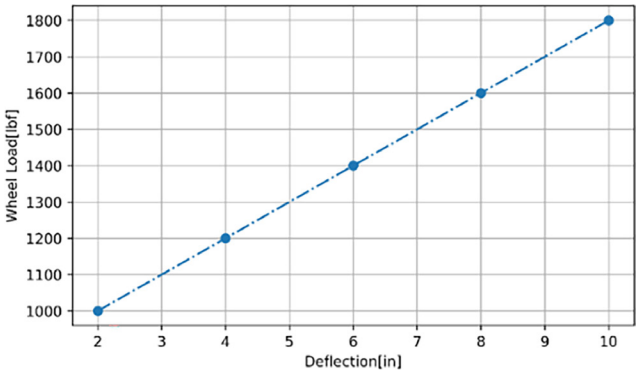

Fig. 13 Performance of wheel load

4.4 Comparison of proposed model with previous models

This section highlights the proposed Mathematical Modeling of Corrugated Geogrid and Geocell Reinforced Flexible Pavement Base with Interlayer Shear performance analysis and designed using a finite element model (FEM) using the ABAQUS tool. The proposed system is compared with existing techniques such as LEA, NLEA, EBEGO, BS 8006, CUR 226, ANN, and BT.

The Fig. 14 shows the comparison analysis of fatigue cracking of the proposed analysis with existing methods such as LEA, and NLEA. The fatigue cracking of the proposed system is lower than existing systems. Fatigue cracking of existing methods such as LEA, and NLEA [32] has a value of 500, and 325 respectively. The proposed system has a low fatigue cracking value of 300 compared with LEA and NLEA. In conclusion, the information shows that the suggested system outperforms the current techniques such as LEA and NLEA due to its much lower fatigue cracking values, which indicate better durability and performance under cyclic loading or fatigue conditions.

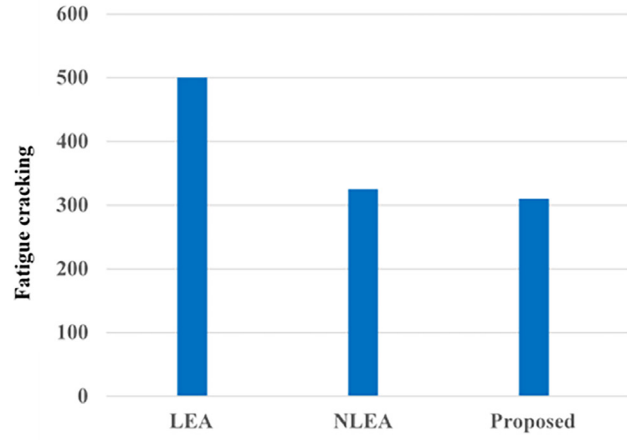

Fig. 14 Comparison of fatigue cracking

The Fig. 15 shows the comparison analysis of rutting of the proposed analysis with existing methods such asLEA, and NLEA. The rutting of the proposed system is lower than existing systems. Rutting of existing methods such as LEA, and NLEA has a value of 600, and 550 respectively. The proposed system has a low rutting value of 500 compared with existing techniques. In comparison to the existing techniques such as LEA and NLEA, the suggested system, shows a lower rutting value, indicating improved performance in preventing the formation of depressions on the road surface. In general, lower rutting levels are preferable since they indicate improved pavement system performance and longevity under traffic loads.

The Fig. 16 shows the comparison analysis of load efficiency of the proposed analysis with existing methods such as EBEGO, BS 8006, and CUR 226 [33]. The load efficiency of the proposed system is higher than existing systems. Load efficiency of existing methods such as EBEGO, BS 8006, and CUR 226 has a value of 80%, 54%, and 81% respectively. The proposed system has a better load efficiency of 83%. In conclusion, the comparative analysis shows that the suggested system outperforms the current approaches (EBEGO - 80%, BS 8006 - 54%, and

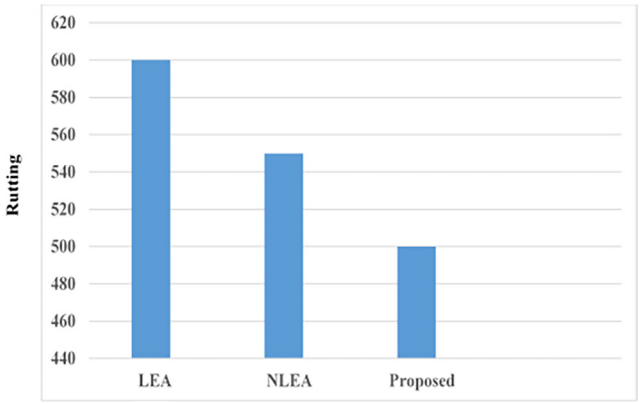

Fig. 15 Comparison of rutting

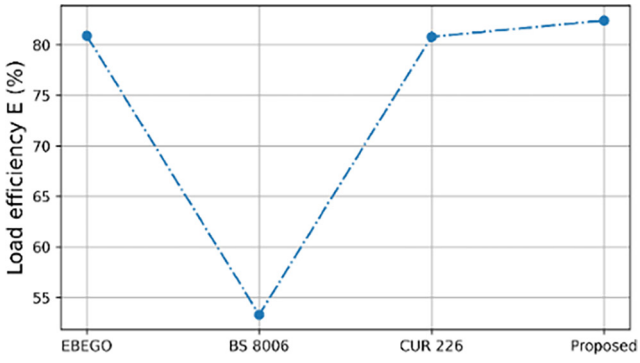

Fig. 16 Comparison of load efficiency

CUR 226 - 81%), with a load efficiency of 83%. This data is essential for evaluating and choosing the best load-supporting strategy in the current situation.

The Fig. 17 shows the comparison analysis of crushing of the proposed analysis with existing methods such as LEA and NLEA. The crushing of the proposed system is lower than the existing techniques. The crushing of LEA and NLEA has a value of 510 and 580 respectively. Whereas the proposed system has a value of 465 which is a lower value compared to existing techniques. In conclusion, based on the reduced crushing value obtained in the analysis, the suggested method is given as having a more favorable or superior crushing performance compared to the current techniques, such as LEA and NLEA [32]. When limiting crushing is a desired result, as in some engineering or materials science applications, lower crushing values typically indicate better results.

The Fig. 18 shows the comparison analysis of load efficiency of the proposed analysis with existing methods such as ANN, and BT. The tensile strain of the proposed system is higher than existing systems. The tensile strain of existing methods such as ANN, and BT [34, 35] has a value of 76 and 90 respectively. The proposed system has a better load efficiency of 115. With a tensile strain of 115, the comparison study concludes that the recommended system performs better than the existing methods. To assess and select the most effective load-supporting approach in the given scenario, this data is important.

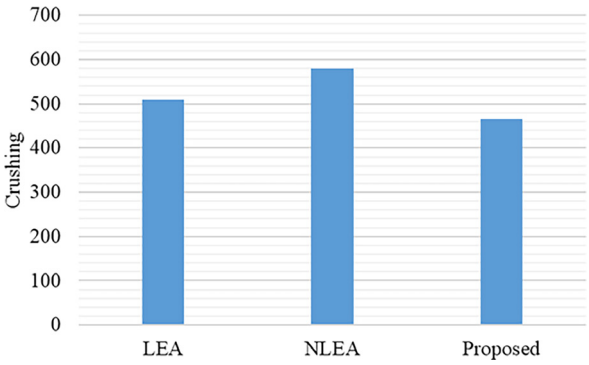

Fig. 17 Comparison of crushing

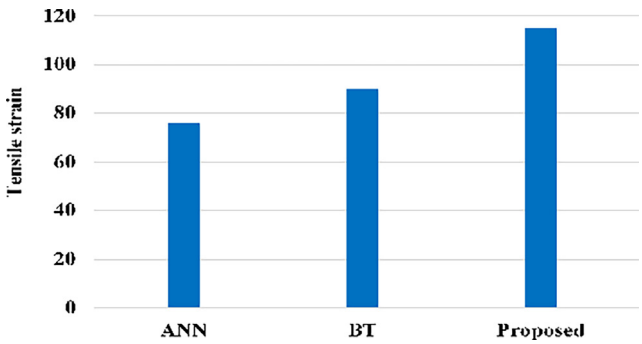

Fig. 18 Comparison of tensile strain

Overall the suggested system performs more efficiently under load than existing methods such as EBEGO, BS 8006, and CUR 226. This suggests that load management is improved with the new design. When compared to existing methods such as LEA and NLEA, it is seen that the suggested approach has low levels of fatigue cracking and rutting. The proposed analysis outperforms existing methods like ANN and BT in load efficiency, with higher tensile strain compared to current systems. This suggests that under repeated load, the new system is less likely to develop cracks and deformations over time, making it a better option overall. The result implies that the suggested approach outperforms current methods when all parameters (fatigue cracking, rutting, and load efficiency, and tensile strain) are taken into account.

5 Conclusions

In this research, a novel Corrugated Imminent Hexagonal Composite Geogrid has been proposed to develop the flexible pavement design to prevent the permanent deformation failure of the flexible pavement and increase its lifetime. The high-strength steel coated with polypropylene increases the friction coefficient between the geogrid and layer material and provides healthier inter-layer bonding and geogrid provides additional shoving resistance and mitigates the failure of the flexible pavement's shoving. This proposed system achieves a higher load efficiency of 83%. Compared with existing techniques proposed system has a less rutting of 500 and fatigue cacking of 310. The proposed flexible pavement design has a better performance of deformation of 56 and shear stress of 0.24 MPa when the number of loads is 1000 and it has a better wheel load, and fatigue damage lifetime. Compared to existing methods the proposed system achieves a lower crushing value of 465 and a higher tensile strain value of 115. The proposed simulation analyses an effective mathematical modeling strategy that uses ABAQUS' finite element model. This proves that the proposed system performed well when compared to other existing techniques such as EBEGO, BS 8006, CUR 226, LEA, and NLEA.

References

[1] Wang, T., Weng, Y., Cai, X., Li, J., Xiao, F., Sun, G., Zhang, F. "Statistical modeling of low-temperature properties and FTIR spectra of crumb rubber modified asphalts considering SARA fractions", Journal of Cleaner Production, 374, 134016. https://doi.org/10.1016/j.jclepro.2022.134016

[2] Jiang, X., Gabrielson, J., Titi, H., Huang, B., Bai, Y., Polaczyk, P., Hu, W. Zhang, M., Xiao, R. "Field investigation and numerical analysis of an inverted pavement system in Tennessee, USA", Transportation Geotechnics, 35, 100759. https://doi.org/10.1016/j.trgeo.2022.100759

[3] Ma, Y., Wang, S., Zhou, H., Hu, W., Polaczyk, P., Huang, B. "Recycled polyethylene and crumb rubber composites modified asphalt with improved aging resistance and thermal stability", Journal of Cleaner Production, 334, 130102, 2022. https://doi.org/10.1016/j.jclepro.2021.130102

[4] Zadehmohamad, M., Luo, N., Abu-Farsakh, M., Voyiadjis, G. "Evaluating long-term benefits of geosynthetics in flexible pavements built over weak subgrades by finite element and Mechanistic-Empirical analyses", Geotextiles and Geomembranes, 50(3), pp. 455–469, 2022. https://doi.org/10.1016/j.geotexmem.2022.01.004

[5] Zhang, L., Peng, B., Xu, Z., Zhou, S. "Shear performance of geosynthetic-encased stone column based on 3D-DEM simulation", Computers and Geotechnics, 151, 104952, 2022. https://doi.org/10.1016/j.compgeo.2022.104952

[6] Vyas, V., Singh, A. P., Srivastava, A. "Prediction of asphalt pavement condition using FWD deflection basin parameters and artificial neural networks", Road Materials and Pavement Design, 22(12), pp. 2748–2766, 2021. https://doi.org/10.1080/14680629.2020.1797855

[7] Aju, D. E., Onyelowe, K. C., Alaneme, G. U. "Constrained vertex optimization and simulation of the unconfined compressive strength of geotextile reinforced soil for flexible pavement foundation construction", Cleaner Engineering and Technology, 5, 100287, 2021. https://doi.org/10.1016/j.clet.2021.100287

[8] Raja, M. N. A., Shukla, S. K., Khan, M. U. A. "An intelligent approach for predicting the strength of geosynthetic-reinforced subgrade soil", International Journal of Pavement Engineering, 23(10), pp. 3505–3521, 2022. https://doi.org/10.1080/10298436.2021.1904237

[9] Wang, T., Dra, Y. A. S. S., Cai, X., Cheng, Z., Zhang, D., Lin, Y., Yu, H. "Advanced cold patching materials (CPMs) for asphalt pavement pothole rehabilitation: State of the art", Journal of Cleaner Production, 366, 133001, 2022. https://doi.org/10.1016/j.jclepro.2022.133001

[10] Zhang, Y., Wang, Y., Wu, Z. G., Lu, Y. M., Kang, A. H., Xiao, P. "Optimal design of geopolymer grouting material for semi-flexible pavement based on response surface methodology", Construction and Building Materials, 306, 124779, 2021. https://doi.org/10.1016/j.conbuildmat.2021.124779

[11] Liu, M., Han, S., Shang, W., Qi, X., Dong, S., Zhang, Z. "New polyurethane modified coating for maintenance of asphalt pavement potholes in winter-rainy condition", Progress in Organic Coatings, 133, pp. 368–375, 2019. https://doi.org/10.1016/j.porgcoat.2019.04.059

[12] Sridhar, R., Guruprasad, H. C., Naveenkumar, D. T., Sangeetha, D. M. "Influence of treated coir fiber on durability properties of black cotton soil", Materials Today: Proceedings, 80, pp. 1611–1616, 2023. https://doi.org/10.1016/j.matpr.2023.02.127

[13] Banerji, A. K., Topdar, P., Datta, A. K. "Structural Performance of Cement-treated Base Layer by Incorporating Reclaimed Asphalt Material and Plastic Waste", Jordan Journal of Civil Engineering, 17(2), pp. 259–271, 2023. https://doi.org/10.14525/JJCE.v17i2.08

[14] Srinivas, A., Balakrishna, P. "Reinforced Flexible Pavement Design Over Clayey Subgrades", [pdf] Journal of Engineering Sciences, 14(03), pp. 260–272, 2023. Available at: https://jespublication.com/upload/2023-V14I3028.pdf

[15] Jelušič, P., Žlender, B. "Parametric analysis of the minimum cost design of flexible pavements", Ain Shams Engineering Journal, 14(2), 101840, 2023. https://doi.org/10.1016/j.asej.2022.101840

[16] Medjdoub, A., Abdessemed, M. "Tests on the Influence of Cyclic Loading and Temperature on the Behaviour of Flexible Pavement Reinforced by Geogrids with Numerical Simulation", Tehnički vjesnik, 30(2), pp. 521–529, 2023. https://doi.org/10.17559/TV-20220806010532

[17] Chua, B. T., Nepal, K. P., Abuel-Naga, H. "Estimating the Bearing Capacity of a Square Footing on a Geogrid-Stabilised Granular Layer over Clay Using the Finite Element Method", Advances in Civil Engineering, 2023, 3560697, 2023. https://doi.org/10.1155/2023/3560697

[18] El-kady, M. S., Azam, A., Yosri, A. M., Nabil, M. "Modelling of railway embankment stabilized with geotextile, geo-foam, and waste aggregates", Case Studies in Construction Materials, 18, e01800, 2023. https://doi.org/10.1016/j.cscm.2022.e01800

[19] Zhang, B., Song, F., Li, W. "Stability Analysis of Retaining Walls with Geocell-Reinforced Road Milling Materials", Sustainability, 15(5), 4297, 2023. https://doi.org/10.3390/su15054297

[20] Ruiz, M., Ramírez, L., Navarrina, F., Aymerich, M., López-Navarrete, D. "A Mathematical Model to Evaluate the Impact of the Maintenance Strategy on the Service Life of Flexible Pavements", Mathematical Problems in Engineering, 2019, 9480675, 2019. https://doi.org/10.1155/2019/9480675

[21] Yin, Z., Ndiema, K. M., Lekalpure, R. L., Kiptum, C. K. "Numerical Study of Geotextile-Reinforced Flexible Pavement Overlying Low-Strength Subgrade", Applied Sciences, 12(20), 10325, 2022. https://doi.org/10.3390/app122010325

[22] Wang, X., Zhang, X., Zhu, Y., Su, T., Li, X. "Full-Scale Field Investigation of Asphalt Pavements Reinforced with Geocells", Transportation Research Record: Journal of the Transportation Research Board, 2675(1), pp. 269–279, 2021. https://doi.org/10.1177/03611981209620

[23] Liu, Z., Gu, X., Ren, H., Wang, X., Dong, Q. "Three-dimensional finite element analysis for structural parameters of asphalt pavement: A combined laboratory and field accelerated testing approach", Case Studies in Construction Materials, 17, e01221, 2022. https://doi.org/10.1016/j.cscm.2022.e01221

[24] Beyene, M. H. "Analysis Of Stress-Strain And Deflection In Flexible Pavements Using Finite Element Method", PhD thesis, Hawassa University, 2022. [online] Available at: http://dlib.hu.edu.et//handle/123456789/3027

[25] Menon, A. R., Bhasi, A., Konnur, S. "Experimental and Numerical Investigation of Column-Supported Soft Clays Reinforced with Basal Geocell", Transportation Infrastructure Geotechnology, pp. 1–28, 2023. https://doi.org/10.1007/s40515-023-00293-3

[26] Matveev, S. A., Martynov, E. A., Litvinov, N. N., Kadisov, G. M., Utkin, V. A. "The geogrid-reinforced gravel base pavement model", Magazine of Civil Engineering, 94(2), pp. 21–30, 2020. https://doi.org/10.18720/MCE.94.3

[27] Mahgoub, A., El Naggar, H. "Coupled TDA–geocell stress-bridging system for buried corrugated metal pipes", Journal of Geotechnical and Geoenvironmental Engineering, 146(7), 04020052, 2020. https://doi.org/10.1061/(ASCE)GT.1943-5606.0002279

[28] Saride, S., Baadiga, R., Balunaini, U., Madhira, M. R. "Modulus Improvement Factor-Based Design Coefficients for Geogrid-and Geocell-Reinforced Bases", Journal of Transportation Engineering, Part B: Pavements, 148(3), 04022037, 2022. https://doi.org/10.1061/JPEODX.0000380

[29] Khorsandiardebili, N., Ghazavi, M. "Static stability analysis of geocell-reinforced slopes", Geotextiles and Geomembranes, 49(3), pp. 852–863, 2021. https://doi.org/10.1016/j.geotexmem.2020.12.012

[30] Sitharam, T. G., Gupta, A. "Interference Effect of Footings on Geocell and Geogrid-Reinforced Clay Beds", In: Sitharam, T. G., Hegde, A. M., Kolathayar, S. (eds.) Geocells: Advances and Applications, Springer, 2020, pp. 173–198. ISBN 978-981-15-6094-1 https://doi.org/10.1007/978-981-15-6095-8_7

[31] Ari, A., Misir, G. "Three-dimensional numerical analysis of geocell reinforced shell foundations", Geotextiles and Geomembranes, 49(4), pp. 963–975, 2021. https://doi.org/10.1016/j.geotexmem.2021.01.006

[32] Dararat, S., Kongkitkul, W., Posribink, T., Jongpradist, P. "Comparison of the lifetime predicted by elastic analyses between two pavement structure candidates considering truck overloading", Road Materials and Pavement Design, 23(5), pp. 1129–1156, 2022. https://doi.org/10.1080/14680629.2021.1883463

[33] Alsirawan, R., Koch, E., Alnmr, A. "Proposed Method for the Design of Geosynthetic-Reinforced Pile-Supported (GRPS) Embankments", Sustainability, 15(7), 6196, 2023. https://doi.org/10.3390/su15076196

[34] Wang, H., Xie, P., Ji, R., Gagnon, J. "Prediction of airfield pavement responses from surface deflections: comparison between the traditional backcalculation approach and the ANN model", Road Materials and Pavement Design, 22(9), pp. 1930–1945, 2021. https://doi.org/10.1080/14680629.2020.1733638

[35] Wang, R., Li, Y., Lv, D., Zhao, W., Zhang, C., Zachert, H., Eichhoff, G., Beroya-Eitner, M. A. "Comparison of Test Methods for Determining the Tensile Strength of Soil and Weak Rocks", Frontiers in Earth Science, 10, 835851, 2022. https://doi.org/10.3389/feart.2022.835851